Impact of Attenuation Correction by Simultaneous Emission/Transmission Tomography on Visual Assessment of ^{201}Tl Myocardial Perfusion Images

Renaud Vidal, Irène Buvat, Jacques Darcourt, Octave Migneco, Philippe Desvignes, Marcel Baudouy and Françoise Bussière

Service de Médecine Nucléaire, Centre Antoine Lacassagne-Laboratoire de Biophysique et de Traitement de l'Image, Université de Nice-Sophia Antipolis, Nice; Service de Cardiologie, Centre Hospitalier Universitaire de Nice, Nice; and U494 INSERM, Centre Hospitalier Universitaire Pitié-Salpétrière, Paris, France

It has been shown in clinical studies that for subjects with a low likelihood of coronary artery disease (CAD), attenuation correction (AC) improves the specificity of defect detection in the inferior wall (right coronary artery [RCA] region). The aim of this study was to investigate the effect of AC on the visual interpretation of the RCA and anteroseptal (corresponding to the left anterior descending artery [LAD]) regions in CAD patients. **Methods:** Fifty-six patients with suspected CAD underwent ^{201}Tl stress/4 h-delayed imaging SPECT using a simultaneous ^{201}Tl emission/^{99m}Tc transmission imaging protocol. Images were reconstructed using the maximum likelihood-expectation maximum algorithm without and with AC. The stress/4 h-delayed images were interpreted blindly for reversible or fixed defects in the RCA and LAD regions by three experienced physicians. Coronary angiography, electrocardiography and enzyme findings were used to establish diagnoses of ischemia or infarction, and receiver operating characteristic (ROC) analyses were performed. **Results:** Statistical testing of ROC curve areas showed that defect detection performance improved with AC when compared with performance without AC in the RCA region. This was mainly the result of a systematic increase in specificity of 12% or more (for any observer and any type of defect) for a similar sensitivity (no definite change in sensitivity values). However, defect detection performance significantly decreased in the LAD territory with AC images ($P < 0.05$) because of a systematic decrease in sensitivity of 20% or more, with no consistent change in specificity. Similar trends were observed when reversible and fixed defects were considered separately. **Conclusion:** AC significantly affects the visual interpretation of ^{201}Tl stress/4 h-delayed SPECT images. This study confirmed the increase in specificity obtained with AC in the RCA territory. However, in the population considered, the studied AC was deleterious for the LAD territory assessment.

Key Words: attenuation correction; ^{201}Tl cardiac SPECT; receiver operating characteristic analysis; coronary artery disease

J Nucl Med 1999; 40:1301–1309

Received Aug. 10, 1998; revision accepted Mar. 12, 1999.

For correspondence or reprints contact: Jacques Darcourt, MD, PhD, Laboratoire de Biophysique et Traitement de l'Image, Faculté de Médecine, 28 Avenue de Valombrose, 06107 Nice Cedex 2, France.

It is now well established that ^{201}Tl SPECT is a valuable tool for the detection and localization of coronary artery disease (CAD) (*1*). However, nonuniform photon attenuation in the chest can cause significant artifacts. It can result in a relative count decrease in the inferior wall, as a result of diaphragmatic attenuation, and in female patients can also introduce a count decrease in the anterior wall as a result of breast attenuation (*2–5*). These patient-specific artifacts increase the number of false-positive cases, thereby reducing ^{201}Tl myocardial SPECT specificity. ^{201}Tl cardiac SPECT is therefore a good candidate for assessing the clinical value of attenuation correction (AC). Because of the large heterogeneity of tissue density in the chest, AC in cardiac SPECT requires measurement of the patient specific map of attenuation coefficients (micro map). Transmission devices allowing micro map acquisition are now becoming clinically available, in addition to AC methods that use these maps (*6,7*). The potential benefit of nonuniform AC in ^{201}Tl cardiac SPECT has been demonstrated in simulations and phantom experiments (*8,9*). However, only a few full reports assess the value of AC in patient series (*10–14*). Kluge et al. (*12*) used ^{99m}Tc-tetrofosmin but considered only patients with abnormalities of the vessels supplying the inferoposterior wall segments. Ficaro et al. (*11*) used a dual-isotope protocol with ^{201}Tl rest study and ^{99m}Tc sestamibi stress imaging to study a population of patients including various types of CAD. However, only the stress study was considered in the analysis, and the evaluation of defect reversibility was not addressed. With ^{201}Tl imaging, Ficaro et al. (*10*) and Prvulovich et al. (*13*) studied only volunteers or patients with low likelihood of CAD. Gallowitsch et al. (*14*) reported increased sensitivity and specificity of lesion detection with AC using nonblinded visual analysis and semiquantitative analysis. They found that AC had a significant impact on the assessment of the severity and extent of myocardial ischemia but, surprisingly, concluded that noncorrected and AC images should be interpreted in a complementary manner so as not to misinterpret studies. The purpose of this study was to determine the impact of nonuniform AC on the visual

interpretation of ^{201}Tl stress/4 h-delayed cardiac images for patients with various degrees of CAD. A nonuniform AC using a currently available simultaneous emission/transmission imaging protocol was considered, and the results were analyzed using the receiver operating characteristic (ROC) methodology.

MATERIALS AND METHODS

Patients

Two-hundred-fifty patients referred for stress ^{201}Tl myocardial perfusion imaging in our hospital between January 1, 1996, and March 15, 1996, were retrospectively considered. Only those patients who underwent coronary angiography within 3 mo of SPECT scans were included. Any patient who suffered a coronary event between the angiographic and SPECT scans were excluded. These criteria resulted in a group of 56 patients (46 men, 10 women; age range 59 ±10 y).

Cardiological Evaluation

Coronary angiography was performed using a standard percutaneous Seldinger technique and was interpreted by two experienced physicians. Three vessels were analyzed: left anterior descending artery (LAD) with diagonal branches, right coronary artery (RCA) and left circumflex artery (LCx). Left ventricular wall motion was studied on the 30° right anterior oblique and 60° left anterior oblique angiographic views. Significant stenosis was defined as ≥70% luminal diameter reduction, with normal wall motion on ventricular angiography. When the angiographic results were retrieved for this study, diagonal branches were included in the LAD territory, and this region was associated with the anteroseptal wall for comparison with SPECT. The inferior wall was associated with the RCA. The lateral wall was assigned to the LCx. The presence of electrocardiographic Q-waves and the elevation of creatine phosphokinase (CPK) enzymes were used to document myocardial infarctions (MIs). Electrocardiographic Q-waves and elevation of CPK enzymes, together with evidence of an akinetic segment supplied by a major epicardial vessel with thrombosis (without collateral blood flow), were necessary to diagnose MI. Because only eight LCx significant abnormalities (one thrombosis and seven stenoses with no LCx one-vessel disease) were found in this study population, the corresponding lateral territory was excluded from the analysis.

Stress/Reinjection Perfusion Imaging

During bicycle ergometry or pharmacological stress (dipyridamole 0.56 mg/kg body weight), 111 MBq (3 mCi) ^{201}Tl were administered intravenously. No patient received β-blockers during the 48 h preceding the study, but nitrates and calcium antagonists were not discontinued. For pharmacological stress, patients had abstained from caffeine and aminophylline for at least 24 h before the test. Dipyridamole was injected intravenously during a period of 4 min, and ^{201}Tl was injected 3 min later. For exercise testing, all patients reached at least 85% of their age-adjusted maximal heart rate ([220 − y of age]min^{-1}). ^{201}Tl was injected at the maximal exercise level, 1 min before ending exercise. For both pharmacological and exercise testing, a reinjection protocol was used for delayed imaging: 37 MBq (1 mCi) ^{201}Tl were injected at rest 4 h after the stress, and the SPECT acquisition was repeated.

Acquisition Protocol

Emission and transmission data were acquired simultaneously for each scan (stress and 4 h delayed) using the dedicated STEP system of a Picker Prism 3000 XP triple-head camera (Picker International, Cleveland, OH) (*15*). Each detector was equipped with a high-resolution fanbeam collimator (CardioFan, focus 65 cm; Picker International). The camera bed was offset so that the heart was positioned close to the center of the camera field of view, and a noncircular orbit was used.

For the transmission scan, the line source located at a fixed focal distance from the opposed collimator was filled with 888 MBq (24 mCi) ^{99m}Tc. The ^{99m}Tc line source was shielded, shuttered and collimated to the size and shape of the opposite collimator and was attenuated with tin plates to maintain a counting rate between 90 and 140 kct/s during the day. A 10-million-count blank scan was acquired every day for transmission calibration. Transmission and emission data were acquired simultaneously in step-and-shoot mode, using 60 projections over 360° (6° angular steps). The times per projection were 16 and 20 s for the stress and delayed scans, respectively. Each head acquired two datasets in two different energy windows: a 15% energy window centered on 140 keV for ^{99m}Tc transmission events and a 30% energy window centered on 73 keV for collecting ^{201}Tl photons. All data were acquired in a 64 × 64 format (pixel size 3.75 × 5 mm). The total emission counts per projection angle ranged from 30 to 100 kct, and the statistics in transmission projection were highly dependent on patient morphology and angle of projection.

Data Processing

^{99m}Tc Attenuation Maps. Before reconstructing the transmission images, ^{201}Tl crosstalk was removed from the transmission data, using the counts recorded in the ^{99m}Tc energy window of the two heads dedicated to emission acquisitions (*8,15*). Transmission data were obtained using fanbeam geometry and could be truncated. The truncation artifacts were minimized by using a finite support constraint when reconstructing the attenuation map (*8*). Reconstruction was performed using 20 iterations of the maximum likelihood-expectation maximum (MLEM) algorithm (*16*). Finally, the ^{99m}Tc attenuation coefficients were scaled to the ^{201}Tl energy, using a linear relationship (*17*):

$$\mu_{Tl}^{201} = 1.05\mu_{Tc}^{99m}.$$

^{201}Tl Emission Images. The ^{201}Tl projections were corrected first for ^{99m}Tc crosstalk (*8,18*) and then reconstructed using 20 iterations of the MLEM algorithm without and with AC. When correcting, attenuation was modeled in the projection/backprojection operators using the previously reconstructed transmission maps. For each reconstruction (without and with AC), two datasets were considered: the reconstructed transaxial slices and these same slices postfiltered by a three-dimensional Wiener filter, as suggested by the manufacturer (Picker International). The reconstructed slices were reoriented into short axis, vertical long axis and horizontal long axis and zoomed for display. The final pixel size was 2.35 × 2.35 mm, and the slice thickness was 4.7 mm.

Four reconstructed datasets for each patient study corresponded to: (a) reconstruction without AC (NC); (b) same as a, followed by a Wiener postfiltering (NC + W); (c) reconstruction with AC using the transmission attenuation map (AC); and (d) same as c, followed by Wiener postfiltering (AC + W).

Visual Analysis

A standard display, presenting stress and the corresponding 4 h delayed slices in the vertical long-axis plane, horizontal long-axis plane and short-axis plane, was considered for visual analysis using a rainbow color scale with a 62% threshold between red and yellow

levels. Because there were 56 patients and four processing methods, 56 × 4 plates were analyzed.

The image plates were analyzed independently on the computer screen by three nuclear medicine physicians unaware of the electrocardiographic findings, clinical information and other imaging results. The observers were asked to consider three regions: the inferior region supplied by the RCA, the anteroseptal region supplied by the LAD and the lateral wall supplied by the LCx. However, as noted, the lateral wall was not considered in the final analysis. For each region, two questions were asked: Is there a reversible defect, and is there a fixed defect? Each diagnosis was given using a five-point rating scale (1 = certainly not, 2 = probably not, 3 = undetermined, 4 = probably yes and 5 = certainly yes). A third score equal to the maximum value of the two scores given for the two questions was subsequently assigned automatically to the detection of a perfusion defect whatever its type (reversible or fixed). This third score, therefore, answered the virtual question "is there any defect?", without considering the nature (fixed or reversible) of the defect.

The results of the visual analysis were compared with the cardiological findings, used as the reference, to perform ROC analyses. A reversible defect was considered true-positive if angiography demonstrated a stenosis ≥70%, with normal wall motion in the corresponding territory. A fixed defect was considered true-positive if there was cardiological evidence of MI in the corresponding territory according to the previously defined criteria. ROC curves were calculated for each question, each observer, each of the two regions (LAD and RCA) and each of the four processing methods, yielding 3 × 3 × 2 × 4 or 72 ROC curves.

Statistical Analysis

The significance of the differences between ROC curves was tested by comparing the areas under the ROC curves (AUCs), using a nonparametric approach accounting for multiple comparisons as described by DeLong et al. (*19*). In this approach, the contrast matrix L was designed according to the hypothesis to be tested. For testing the effect of Wiener postfiltering in a given region (LAD or RCA), a θ vector of AUC, with components $\{\theta i\}_{i=1,9}$, was defined by: θ1, θ5, θ9 = AUC for observers 1–3, respectively, interpreting NC images; θ2, θ6, θ10 = AUC for observers 1–3, respectively, interpreting NC + W images; θ3, θ7, θ11 = AUC for observers 1–3, respectively, interpreting AC images; and θ4, θ8, θ12 = AUC for observers 1–3, respectively, interpreting AC + W images. The associated contrast matrix L was:

$$L(i,j) = \begin{cases} -1 \text{ if } j = 2i - 1 \\ 1 \text{ if } j = 2i \\ 0 \text{ otherwise} \end{cases} \quad i \in [1,6], j \in [1,12].$$

The test resulted in a χ^2 value with 6 degrees of freedom (df).

For testing the effect of attenuation correction in the RCA and LAD territories, for each type of defect, a θ vector of AUC, with components $\{\theta i\}_{i=1,6}$, was defined by: θ1, θ3, θ5 = AUC for observers 1–3, respectively, interpreting NC images and θ2, θ4, θ6 = AUC for observers 1–3, respectively, interpreting AC images. The contrast matrix L was:

$$L(i,j) = \begin{cases} -1 \text{ if } j = 2i - 1 \\ 1 \text{ if } j = 2i \\ 0 \text{ otherwise} \end{cases} \quad i \in [1,3], j \in [1,6].$$

The test resulted in a χ^2 value with 3 df. For all tests, the significance level was set at $P < 0.05$.

RESULTS

Patients

There were 22 healthy patients and 19, 13 and 2 patients with one-, two- and three-vessel disease, respectively. The nature and localization of the lesions are given in Table 1.

Effect of Wiener Postfiltering

The AUC obtained when interpreting images for any kind of abnormality (i.e., considering the answer to the third virtual question: "is there any defect?") without and with Wiener filtering are given in Table 2.

When testing whether Wiener filtering significantly affected the detectability of defects in the LAD region, the χ^2 value with 6 df was 19.65, indicating that Wiener filtering significantly reduced defect detectability as measured by AUC ($P < 0.005$). Given the overall significant difference, the AUC observed without and with Wiener filtering were compared for each observer independently (using L = [−1,1]). The AUC was significantly lower with Wiener filtering than without in two instances, and none of the four other differences was significant.

In the RCA region, the χ^2 value with 6 df was 8.93, meaning that Wiener filtering did not significantly affect defect detectability.

Because these results did not provide evidence that Wiener filtering improved defect detectability, subsequent analyses were performed using the scores observed for NC and AC images that were not postfiltered using the Wiener filter.

Effect of Attenuation Correction in the Right Coronary Artery Region

The AUC obtained for different observers when interpreting the RCA region are given in Table 3. The AUC was

TABLE 1
Angiographic Findings

Coronary artery lesions	Insignificant disease	One-vessel disease	Two-vessel disease	Three-vessel disease
Number of patients	22	19	13	2
LAD stenoses	—	6	10	2
LAD thromboses with MI	—	5	2	0
RCA stenoses	—	5	5	1
RCA thromboses with MI	—	3	3	1
LCx stenoses	—	0	5	2
LCx thromboses with MI	—	0	1	0

LAD = left anterior descending artery; MI = myocardial infarction; RCA = right coronary artery; LCx = left circumflex artery.

TABLE 2
Receiver Operator Characteristic Curve Areas for Three Observers Detecting Lesions on Images (Reversible or Fixed Defects), Without and With Wiener Postfiltering

Region	Observer	Without AC		With AC	
		Without Wiener	With Wiener	Without Wiener	With Wiener
LAD	1	0.69 ± 0.07	0.59 ± 0.08*	0.63 ± 0.08	0.70 ± 0.07
	2	0.82 ± 0.06	0.63 ± 0.08†	0.63 ± 0.08	0.65 ± 0.07
	3	0.81 ± 0.06	0.68 ± 0.07	0.65 ± 0.07	0.66 ± 0.07
RCA	1	0.68 ± 0.08	0.66 ± 0.08	0.80 ± 0.07	0.71 ± 0.08
	2	0.69 ± 0.08	0.75 ± 0.07	0.85 ± 0.06	0.76 ± 0.07
	3	0.75 ± 0.08	0.76 ± 0.07	0.83 ± 0.07	0.78 ± 0.07

*Significant difference between without and with Wiener postfiltering at $P < 0.05$.
†Significant difference between without and with Wiener postfiltering at $P < 0.005$.
AC = attenuation correction; LAD = left anterior descending artery; RCA = right coronary artery.

always greater with AC than without for all observers and all questions. Testing the significance of the observed differences, AUC was found to be significantly higher with AC than without for reversible defects ($\chi^2 = 12.64$, 3 df, $P < 0.01$) and fixed defects ($\chi^2 = 10.04$, 3 df, $P < 0.025$), but the test failed to detect a significant difference when all defects were pooled together ($\chi^2 = 7.44$, 3 df, whereas $P < 0.05$ corresponds to $\chi^2 = 7.81$). This means that AC increased the accuracy of the diagnosis (more reversible defects were identified as such, and similarly for the fixed defects). On the other hand, the study population was not large enough to demonstrate that AC also improved the detection of defects when one did not consider their nature (reversible or fixed). For reversible and fixed defects, given the overall significant difference, the significance of the difference of AUC without and with AC was tested for each observer and each type of defect independently, and results are shown in Table 3.

The ROC curves observed for the detection of any defect are shown in Figure 1 , for the three observers, without and with AC. These curves were obtained by plotting the observed (false-positive fraction, sensitivity) couples for the different decision thresholds, without any ROC curve-fitting, to be consistent with the nonparametric nature of the tests that were used to determine the significance of the difference between the curves (*19*). The three curves show that AC images tended to offer a greater detectability than NC images, especially when considering strict or moderate detection thresholds (left part of the curves), whereas the benefit of AC was more disputable for lax detection thresholds (cases called positive if any suspicion of defect, top right part of the curves).

TABLE 3
Receiver Operator Characteristic Curve Areas for Three Observers Interpreting RCA Region for Reversible or Fixed Defects

Question	Observer	Without AC	With AC
Any defect?	1	0.68 ± 0.08	0.80 ± 0.07
	2	0.69 ± 0.08	0.85 ± 0.06
	3	0.75 ± 0.07	0.83 ± 0.07
Reversible defect?	1	0.62 ± 0.10	0.71 ± 0.09
	2	0.38 ± 0.09	0.74 ± 0.09*
	3	0.49 ± 0.10	0.67 ± 0.10
Fixed defect?	1	0.65 ± 0.12	0.74 ± 0.11*
	2	0.73 ± 0.11	0.98 ± 0.04†
	3	0.68 ± 0.12	0.97 ± 0.04†

*Significant difference between without and with AC at $P < 0.01$.
†Significant difference between without and with AC at $P < 0.025$.
RCA = right coronary artery; AC = attenuation correction.

The sensitivity and specificity values measured for the different observers when considering scores 4 and 5 (probably yes and certainly yes) as positive are given in Table 4. This operating point was chosen by maximizing the diagnosis accuracy for each study (each observer, each region and each question) and considering the operating point that maximized the accuracy most often. Sensitivity was not affected consistently by AC, depending on the observer and on the question that was asked. The average sensitivity values among the different observers without and with AC were not greatly different, except when asking for the presence of a fixed defect, for which sensitivity was ~30% higher with AC. Specificity was systematically higher with AC than without AC. The increase in specificity was between +12% and +65% for this region.

Effect of Attentuation Correction in Left Anterior Descending Artery Region

Table 5 shows the AUC for the different observers when considering the LAD region. The AUCs were systematically lower with AC for all observers whatever the question. When testing the significance of the differences, AUC was found to be significantly lower with AC than without for reversible defects ($\chi^2 = 11.88$, 3 df, $P < 0.01$), fixed defects ($\chi^2 = 8.08$, 3 df, $P < 0.05$) and any defect ($\chi^2 = 13.23$, 3 df, $P < 0.005$). These results show that AC actually reduced the detectability of the defects in the LAD region. The significance of the difference of AUC without and with AC for each observer and each type of defect is shown in Table 5.

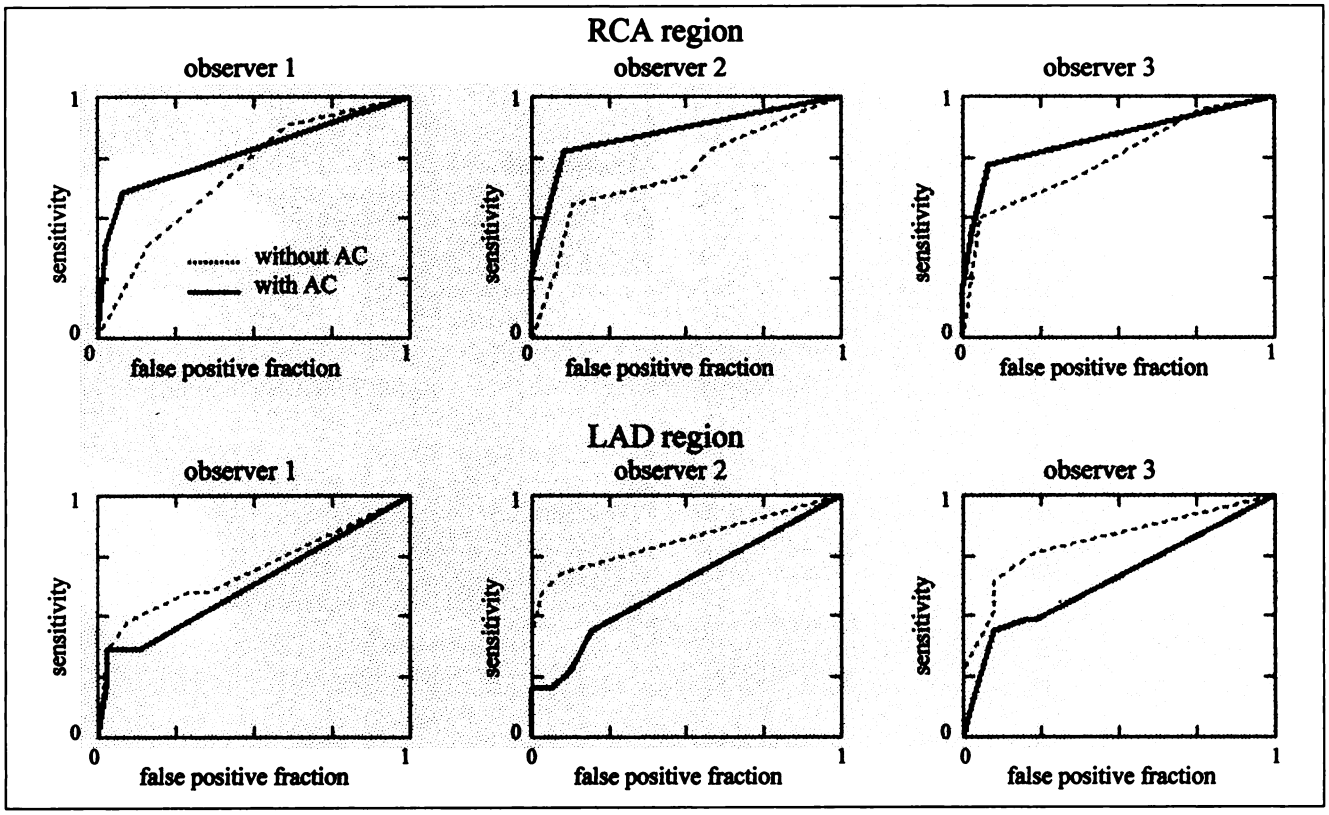

FIGURE 1. ROC curves obtained for three observers when interpreting RCA (top) and LAD (bottom) regions for any defect (reversible or fixed).

The ROC curves observed when considering the detection of any defect without and with AC are shown in Figure 1 for the three observers. These curves show that for any given false-positive fraction, the sensitivity was higher for NC images than for AC images, whereas for any sensitivity value, the false-positive fraction was smaller when using the NC images than when considering the AC images. This suggests that the NC images offered greater detectability of defects in the LAD region for any detection threshold.

Considering scores 4 and 5 as positive, the sensitivity and specificity values for the different observers are given in Table 6. For all questions, sensitivity was reduced with AC by more than 20%. Specificity was not consistently affected and remained similar.

TABLE 4
Sensitivity and Specificity for Three Observers Interpreting RCA Region for Reversible or Fixed Defects

Question	Observer	Sensitivity (%)		Specificity (%)	
		Without AC	With AC	Without AC	With AC
Any defect?	1	89	67	37	90
	2	78	78	42	89
	3	94	72	24	89
	Average	87 ± 7	72 ± 4	34 ± 8	89 ± 1
Reversible defect?	1	73	54	49	87
	2	36	54	49	93
	3	73	45	27	87
	Average	61 ± 17	51 ± 4	42 ± 10	89 ± 3
Fixed defect?	1	57	57	57	90
	2	57	100	84	96
	3	57	100	65	90
	Average	57 ± 1	86 ± 20	69 ± 11	92 ± 3

RCA = right coronary artery; AC = attenuation correction.

TABLE 5
Receiver Operator Characteristic Curve Areas for Three Observers Interpreting LAD Region for Reversible or Fixed Defects

Question	Observer	Without AC	With AC
Any defect?	1	0.69 ± 0.07	0.63 ± 0.08
	2	0.82 ± 0.06	0.63 ± 0.08*
	3	0.81 ± 0.06	0.66 ± 0.07†
Reversible defect?	1	0.61 ± 0.08	0.56 ± 0.08
	2	0.78 ± 0.07	0.58 ± 0.08*
	3	0.75 ± 0.08	0.58 ± 0.08‡
Fixed defect?	1	0.82 ± 0.10	0.69 ± 0.12
	2	0.83 ± 0.10	0.68 ± 0.12
	3	0.98 ± 0.04	0.69 ± 0.12*

*Significant difference between without and with AC at $P < 0.005$.
†Significant difference between without and with AC at $P < 0.025$.
‡Significant difference between without and with AC at $P < 0.05$.
LAD = left anterior descending artery; AC = attenuation correction.

Figure 2 illustrates the results. The patient was a 59-y-old man. Without AC, the study was called positive for reversible defect in the RCA territory by two observers (scores 4) and undetermined by the third observer (score 3). It was also called positive for reversible defect in the LAD territory by two observers (scores 4, 4 and 1). The AC study was considered normal by all observers (scores 1 in the RCA and LAD regions). Coronary angiography showed no significant lesion on the RCA and two ≥70% LAD stenoses. The study was therefore false-positive in the RCA region and true-positive in the LAD region (for two observers) without AC. With AC, it became true-negative in the RCA region and false-negative in the LAD territory. This example also shows the well-known decrease in count intensity at the apex resulting from AC (*10,14*).

DISCUSSION

As emphasized by Hutton (*20*) in a recent editorial, "a large number of individuals remain skeptical of the value of attenuation correction, perhaps, in some respects, rightly so." Although simulations and phantom experiments have demonstrated the potential value of AC (*8,9*), some reports gave evidence that AC can complicate the interpretation of cardiac images (*21,22*), and there is still a controversy whether NC and AC images should be reviewed simultaneously for interpretation (*14,23*). Moreover, there is a lack of data regarding the clinical evaluation of the value of AC, especially in ^{201}Tl imaging (*10,13,14*). Prvulovich et al. (*13*) assessed the value of AC for patients with a low probability of CAD, and Ficaro et al. (*10*) also considered CAD patients for illustrative purposes but did not address the problem of diagnostic benefit of AC for the detection of CAD. Although Gallowitsch et al. (*14*) reported increased sensitivity and specificity values with AC, the authors concluded that NC and AC images should be interpreted in a complementary manner so as not to misinterpret studies, suggesting that the clinical use of AC might raise problematic issues. This study was designed to determine the changes in visual diagnostic interpretation resulting from AC in a clinical situation. Patients with a high probability of CAD were included, and both localization and reversibility of defects were assessed.

The studied population consisted of 56 patients at risk for CAD. No subjects with low likelihood of CAD were included, but 22 patients who underwent coronary angiography had no significant stenosis. Among the 34 patients with significant CAD, 44% had multivessel disease and 50% had thrombosis resulting from MI. Therefore, these results reflect those obtained in a severely diseased population.

We compared the images reconstructed with the iterative MLEM algorithm with and without AC. Other studies compared iteratively reconstructed AC images with NC images reconstructed using filtered backprojection (*10–14*).

TABLE 6
Sensitivity and Specificity for Three Observers Interpreting LAD Region for Reversible or Fixed Defects

		Sensitivity (%)		Specificity (%)	
Question	Observer	Without AC	With AC	Without AC	With AC
Any defect?	1	60	36	64	87
	2	68	44	90	81
	3	76	48	77	77
	Average	68 ± 8	43 ± 5	77 ± 11	82 ± 4
Reversible defect?	1	44	22	71	87
	2	61	33	82	82
	3	67	39	76	74
	Average	57 ± 8	31 ± 6	76 ± 4	81 ± 5
Fixed defect?	1	71	43	86	94
	2	71	43	92	92
	3	100	43	96	94
	Average	81 ± 14	43 ± 1	91 ± 4	93 ± 1

LAD = left anterior descending artery; AC = attenuation correction.

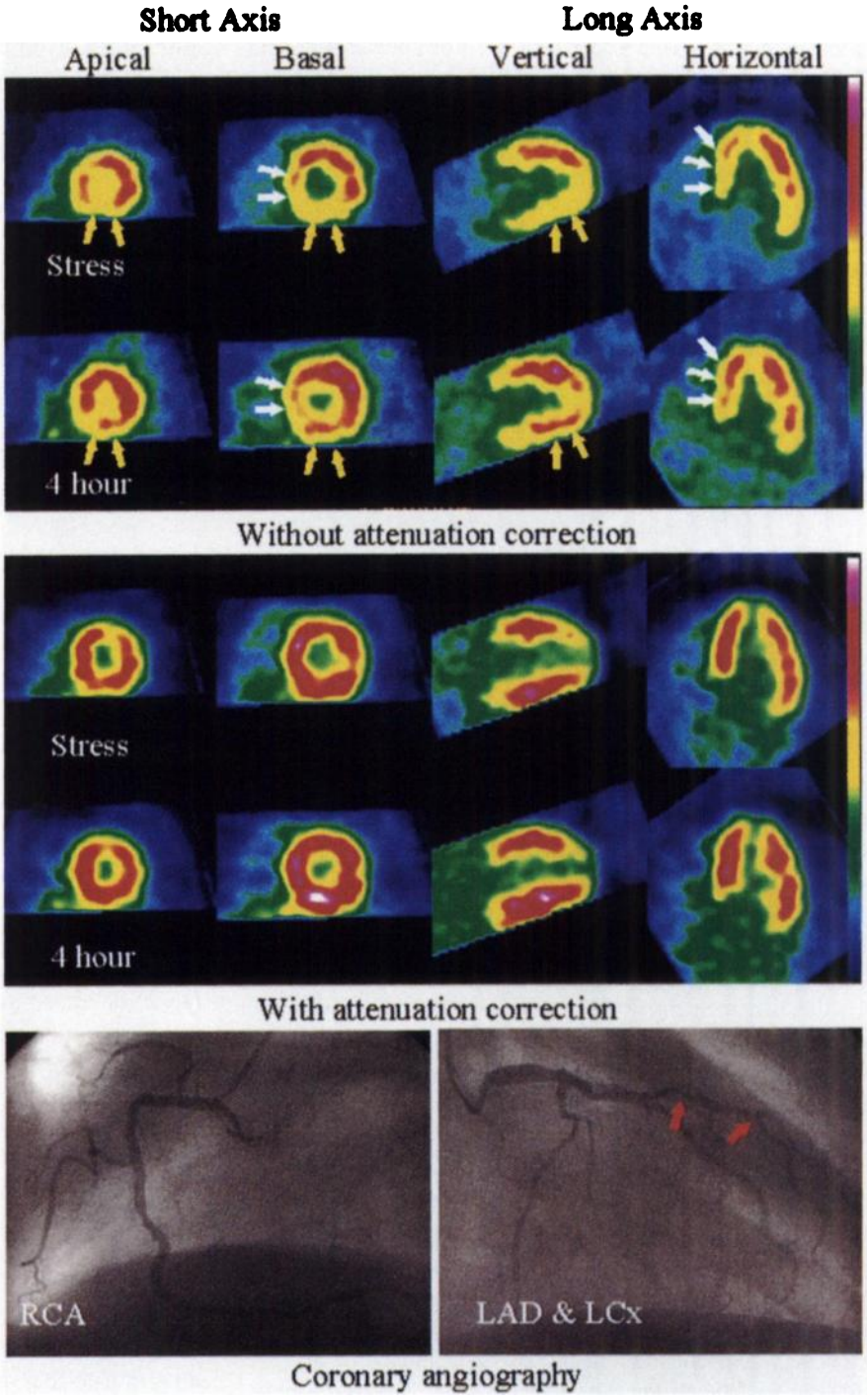

FIGURE 2. Without AC, this 59-y-old man was diagnosed in RCA region (yellow arrows) by two observers as positive for ischemia (scores 4) and by third observer as undetermined (score 3) and was diagnosed as positive for ischemia in LAD territory by two observers (scores 4, 4 and 1) (white arrows). AC study was considered normal (scores 1 by all observers) in all regions. Coronary angiography showed no significant lesion on RCA but revealed two ≥70% LAD stenoses (red arrows). NC study was therefore false-positive for RCA territory and true-positive in LAD territory for two observers. With AC, study was true-negative in RCA region but false-negative in LAD territory. Apical decrease in count density resulting from AC was also seen.

Our method has the advantage of considering the specific effect of AC for a given reconstruction algorithm. For NC and AC data, 20 iterations were used, although the optimal number of iterations might be different depending on whether AC is included. We checked that there was no visual difference between the results obtained after 15 or 20 iterations when no AC was performed and that the results were also similar for 20 or 30 iterations when AC was used.

Only visual image analysis was performed, using the conventional horizontal long-axis, vertical long-axis and short-axis planes, because we do not routinely use bull's-eye display and semiquantitative analysis in our department. The three observers each had 1 y of experience reading AC ^{201}Tl images in stress/4 h-delayed cardiac SPECT using the device considered in this study and were therefore trained in reading such images.

The effect of Wiener postfiltering on image interpretation was investigated first. Postreconstruction filtering is usually recommended (*24,25*). The manufacturer suggested a Wiener filter, because it accounted for the collimator response measured in scattering medium and, therefore, supposedly restored loss of image quality resulting from scatter and

collimator response. In our results with or without AC, the effect of this filtering procedure did not appear beneficial. This is consistent with the lack of diagnosis accuracy improvement with Wiener filtering previously reported for ^{201}Tl cardiac SPECT in women (*26*). Filtering, therefore, was not considered for further evaluation of AC.

When considering the inferior region, it was found that AC resulted in significantly increased performance in properly identifying reversible and fixed defects (Table 3). Although sensitivity and specificity estimates should be interpreted with caution, given the small number of true-positives in each group, they give some evidence that the increase in detection performance was mainly caused by an increased specificity for an equivalent sensitivity (Table 4). This result is consistent with those illustrated by Ficaro et al. (*10*) for a few cases by ^{201}Tl imaging or reported by Kluge et al. (*12*) and Ficaro et al. (*11*) by ^{99m}Tc cardiac SPECT imaging for large groups of CAD patients.

When considering the anteroseptal region, the consequences of AC were completely different (Table 5). For all observers, the overall performance in lesion detection was systematically reduced with AC than without. This was mainly the result of a decrease in lesion detection sensitivity (Table 6), as illustrated in Figure 2. What appeared as a perfusion defect without AC became a near-normal homogeneous uptake with AC and was most often called normal. Such a decrease in defect detection sensitivity has not been demonstrated in previous studies using different acquisition protocols and different evaluation methodologies, but Gallowitsch et al. (*14*) reported a decrease in defect size with AC, which was actually greater in the LAD territory (−36%) than in the RCA region (−23%). The evaluation methodology used by these authors (alternative forced choice for image interpretation and nonblinded study for patients with known CAD) may have in fact obscured a trend toward decreased defect detection sensitivity. The variability of the extent of myocardial perfusion defects in patients with similar anatomic defect severity and location might also partially explain the decrease in sensitivity observed in this study. Indeed, Mahmarian et al. (*27*) reported that this variability was most striking in the anteroseptal region: in patients with ≥70% proximal LAD stenosis, the perfusion defects ranged from as little as 7% to as large as 44% of the left ventricle. The decrease in defect size resulting from AC, therefore, is probably more critical in the LAD territory and could lead to false-negative interpretation in this region. Furthermore, Ficaro et al. (*11*) also found that, unlike in the RCA or LCx regions, AC did not improve image interpretation in the LAD region for stress ^{99m}Tc-sestamibi scans (ROC curve with AC below ROC curve for NC data).

During the reading sessions, observers were also asked to rate the presence of reversible or fixed defects in the apical region, exactly as they did in the inferior and anteroseptal regions (results not shown). When considering scores given for this region only, ROC analyses did not show any significant trend in change of defect detection performance at the apex, even if an apical decrease of activity was seen with AC. This indicates that this apical decrease of activity resulting from AC, which has already been reported (*10,14*), did not adversely affect the visual image interpretation in this region.

The results in terms of detection performance varied among observers. In addition to the intrinsic observer variability, the small number of true-positive cases in each category (Table 1) was responsible for the large range of AUC, sensitivity and specificity values observed for a given group. However, despite this variability, the same trends were observed among all three observers regarding the effect of AC for the two myocardial regions considered. The AUC systematically varied in the same direction between NC and AC data, demonstrating that the changes in visual interpretation caused by AC were consistent among observers.

Our mean values of sensitivity/specificity trade-off for defect detection in the RCA territory ranged from 87%/34% (any type of defect without AC) to 86%/92% (fixed defects with AC). In a multicenter study regarding quantitative analysis of ^{201}Tl stress SPECT images (without considering defect reversibility), Van Train et al. (*28*) reported trade-off values ranging from 82%/33% to 85%/72%. For the detection of defects in the LAD territory, our sensitivity/specificity trade-off values ranged from 31%/81% (reversible defects with AC) to 81%/91% (fixed defects without AC). In this region, Van Train et al. found values ranging from 40%/67% to 79%/86%. Despite the small number of true-positive cases in the different groups (Table 3), our sensitivity and specificity trade-off values were within the range of those found in the literature, except for the sensitivity of AC data in the LAD territory.

Further investigations are necessary to clarify the reasons for the deleterious effect of AC in the LAD territory. Because the previous studies regarding the clinical impact of AC in ^{201}Tl imaging did not use a ^{99m}Tc transmission source, crosstalk might be responsible in part for these results. Potential sources of artifacts, such as absence of scatter correction, respiratory motion, cardiac motion, extra cardiac activity and noise in the attenuation maps, should also be investigated. Meanwhile, these results suggest that when using AC with an imaging protocol similar to ours, AC images probably should be interpreted in conjunction with NC images, and the degree of confidence given to NC and AC data should be weighed appropriately depending on the territory that is considered. For interpreting the inferior wall region, AC images should be trusted more than NC images, whereas when interpreting the anteroseptal region, observations from the NC images should weigh more than observations from the AC images.

CONCLUSION

In a population including severe CAD patients, AC using a simultaneous ^{201}Tl emission/^{99m}Tc transmission protocol significantly affected the visual interpretation of stress/4 h-

delayed cardiac SPECT. Consistent with previous reports, the specificity of reversible- or fixed-defect detection was significantly increased in the inferior wall. However, we found that the sensitivity of defect detection was significantly reduced in the anteroseptal region. Because the reason for this decreased performance in reversible- or fixed-defect detection is not understood yet for this particular imaging protocol, we recommend combined interpretation of AC with NC images and careful evaluation of any simultaneous emission/transmission imaging protocol in patients before using such a protocol on a routine basis.

ACKNOWLEDGMENTS

We thank the nuclear medicine staff for technical assistance in acquiring the studies. We also thank Robert Di Paola and colleagues from U494 INSERM for their helpful discussions in the design of the evaluation protocol. This work was presented in part at the 45th Society of Nuclear Medicine annual meeting in Toronto, Ontario, Canada, June 8–10, 1998.

REFERENCES

1. Mahmarian JJ, Verani MS. Exercise thallium-201 perfusion scintigraphy in the assessment of coronary artery disease. *Am J Cardiol.* 1991;67:2D–11D.
2. Eisner RL, Tamas MJ, Cloninger K. Normal SPECT thallium-201 bull's eye display: gender differences. *J Nucl Med.* 1988;29:1901–1909.
3. DePuey EG, Garcia EV. Optimal specificity of thallium-201 SPECT through recognition of imaging artifacts. *J Nucl Med.* 1989;30:441–449.
4. Manglos SH, Thomas FD, Gagne GM, Hellwig BJ. Phantom study of breast tissue attenuation in myocardial imaging. *J Nucl Med.* 1993;34:992–996.
5. Toft J, Hesse B, Rabol A. The occurrence of false-positive technetium-99m sestamibi bull's eye defects in different reference databases. *Eur J Nucl Med.* 1997;24:179–183.
6. King MA, Tsui BMW, Pan TS. Attenuation compensation for cardiac single-photon emission computed tomographic imaging: part 1. Impact of attenuation and methods of estimating attenuation maps. *J Nucl Cardiol.* 1995;2:513–524.
7. King MA, Tsui BMW, Pan TS, Glick SJ, Soares EJ. Attenuation compensation in cardiac single-photon emission computed tomographic imaging: part 2. Attenuation compensation algorithms. *J Nucl Cardiol.* 1996;3:55–63.
8. Tung CH, Gullberg GT, Zeng GL, Christian PE, Datz FL, Morgan HT. Non-uniform attenuation correction using simultaneous transmission and emission converging tomography. *IEEE Trans Nucl Sci.* 1992;39:1134–1143.
9. Tsui BMW, Zhao XD, Gregoriou GK, et al. Quantitative cardiac SPECT reconstruction with reduced image degradation due to patient anatomy. *IEEE Trans Nucl Sci.* 1994;41:2838–2844.
10. Ficaro EP, Fessler JA, Ackermann RJ, Rogers WL, Corbett JR, Schwaiger M. Simultaneous transmission-emission thallium-201 cardiac SPECT: effect of attenuation correction on myocardial distribution. *J Nucl Med.* 1995;36:921–931.
11. Ficaro EP, Fessler JA, Shreve PD, Kritzman JN, Rose PA, Corbett JR. Simultaneous transmission/emission myocardial perfusion tomography. Diagnostic accuracy of attenuation-corrected ^{99m}Tc-sestamibi single-photon emission computed tomography. *Circulation.* 1996;93:463–473.
12. Kluge R, Sattler B, Seese A, Knapp WH. Attenuation correction by simultaneous emission-transmission myocardial single-photon emission tomography using a technetium-99m-labelled radiotracer: impact on diagnostic accuracy. *Eur J Nucl Med.* 1997;24:1107–1114.
13. Prvulovich EM, Lonn AHR, Bomanji JB, Jarritt PH, Ell PJ. Effect of attenuation correction on myocardial thallium-201 distribution in patients with a low likelihood of coronary artery disease. *Eur J Nucl Med.* 1997;24:266–275.
14. Gallowitsch HJ, Sykora J, Mikosch P, et al. Attenuation-corrected thallium-201 single-photon emission tomography using a gadolinium-153 moving line source: clinical value and the impact of attenuation correction on the extent and severity of perfusion abnormalities. *Eur J Nucl Med.* 1998;25:220–228.
15. Gullberg GT, Morgan HT, Zeng GL, et al. The design and performance of a simultaneous transmission and emission tomography system. *IEEE Trans Nucl Sci.* 1998;3:1676–1698.
16. Lange K, Carson R. EM reconstruction algorithms for emission and transmission tomography. *J Comput Assist Tomogr.* 1984;8:306–316.
17. Tsui BMW, Gullberg GT, Edgerton ER, et al. Correction of nonuniform attenuation in cardiac SPECT imaging. *J Nucl Med.* 1989;30:497–507.
18. Frey EC, Tsui BMW, Perry JR. Simultaneous acquisition of emission and transmission data for improved Tl-201 cardiac SPECT imaging using a Tc-99m transmission source. *J Nucl Med.* 1992;12:2238–2245.
19. DeLong ER, DeLong DM, Clarke-Pearson DL. Comparing the areas under two or more correlated receiver operating characteristic curves: a nonparametric approach. *Biometrics.* 1988;44:837–845.
20. Hutton BF. Cardiac single-photon emission tomography: is attenuation correction enough? *Eur J Nucl Med.* 1997;24:713–715.
21. Heller EN, DeMan P, Liu YH, et al. Extracardiac activity complicates quantitative cardiac SPECT imaging using a simultaneous transmission-emission approach. *J Nucl Med.* 1997;38:1882–1890.
22. Matsunari I, Böning G, Ziegler SI, et al. Attenuation-corrected rest thallium-201/stress Tc-99m sestamibi myocardial SPECT in normals. *J Nucl Cardiol.* 1998;5:48–55.
23. Corbett JR, Duvernoy CS, Fessler JA, Ficaro EP. Attenuation-corrected SPECT perfusion imaging: should corrected and uncorrected images be viewed together? [abstract] *J Nucl Med.* 1998;39:73P.
24. Tausig A, Walser R, Knesewitsch P, et al. Influence of postfiltering on the accuracy of myocardial scintigraphy using nonhomogeneous attenuation correction [abstract]. *Eur J Nucl Med.* 1996;23:1049.
25. Walser R, Tausig A, Knesewitsch P, et al. Effects of patient specific attenuation correction on myocardial SPECT findings in controls [abstract]. *Eur J Nucl Med.* 1996;23:1049.
26. Hansen CL, Kramer M, Rastogi A. Lower diagnostic accuracy of thallium-201 SPECT myocardial perfusion imaging in women not improved by Wiener filtering [abstract]. *J Nucl Med.* 1998;39:46P.
27. Mahmarian JJ, Pratt CM, Boyce TM, Verani MS. The variable extent of jeopardized myocardium in patients with single vessel coronary artery disease: quantification by thallium-201 single photon emission computed tomography. *J Am Coll Cardiol.* 1991;17:355–362.
28. Van Train KF, Maddahi J, Berman DS, et al. Quantitative analysis of tomographic stress thallium-201 myocardial scintigrams: a multicenter trial. *J Nucl Med.* 1990;31:1168–1179.